JACS
JOURNAL OF THE AMERICAN CHEMICAL SOCIETY

COMMUNICATION

pubs.acs.org/JACS

High-Yield Synthesis of Few-Layer Graphene Flakes through Electrochemical Expansion of Graphite in Propylene Carbonate Electrolyte

Junzhong Wang, Kiran Kumar Manga, Qiaoliang Bao, and Kian Ping Loh*

Department of Chemistry, National University of Singapore, 3 Science Drive 3, Singapore 117543

Supporting Information

ABSTRACT: High-yield production of few-layer graphene flakes from graphite is important for the scalable synthesis and industrial application of graphene. However, high-yield exfoliation of graphite to form graphene sheets without using any oxidation process or super-strong acid is challenging. Here we demonstrate a solution route inspired by the lithium rechargeable battery for the high-yield (>70%) exfoliation of graphite into highly conductive few-layer graphene flakes (average thickness <5 layers). A negative graphite electrode can be electrochemically charged and expanded in an electrolyte of Li salts and organic solvents under high current density and exfoliated efficiently into few-layer graphene sheets with the aid of sonication. The dispersible graphene can be ink-brushed to form highly conformal coatings of conductive films (15 ohm/square at a graphene loading of <1 mg/cm^2) on commercial paper.

The chemical synthesis of solution-dispersible graphene has received intense interest[1−9] in the chemical community since the isolation of graphene by the "Scotch tape" method.[10,11] The challenge is to identify a high-yield method that can exfoliate graphite efficiently into solution-dispersible graphene sheets without collateral damage to the graphene. Acid exfoliation of graphite based on the recipe developed by Hummers and Offeman produces solution dispersible graphene oxide (GO) flakes.[12] The presence of oxygen functional groups in these GO flakes helps make them dispersible in solution but destroys their electrical conductivity because of the inevitable disruption of long-range conjugation.[8] Another drawback is that chemical or thermal reduction has to be performed on the GO before electrical conductivity can be recovered, albeit only partially.[8,13] The insulating and defective nature of GO precludes its direct application as an electronic material.[13−15] It is desirable to identify a high-yield method that can directly exfoliate graphite into graphene sheets. There have been numerous attempts to exfoliate graphite by sonicating it in organic solvents in the presence of organic intercalators or surfactants, but usually only the surface layers of graphite were peeled off in a very limited way as opposed to complete exfoliation of the starting reactant.[2−4,16−20] Since the amount of exfoliated product is usually very limited relative to the starting material, the actual yield for producing single-layer graphene (SLG) or few-layer graphene (FLG) is very low, typically less than 1%. Here we present a nonoxidative electrochemical process wherein the application of a sufficiently high current density to a negative graphite electrode results in its exfoliation into FLG flakes. The yield of FLG is larger than 70% relative to the total amount of starting graphite. The electrochemical charging process was investigated in detail to gain insights into the exfoliation process.

The exfoliation method to produce FLG was inspired by the electrochemical reactions of negative graphite electrodes in liquid-rechargeable lithium ion batteries (LIBs). During electrochemical charging in a graphite electrode, Li^+ ions are reversibly intercalated into the graphite interlayers according to a series of well-defined stages. However, loss of reversibility can arise when there is solvent cointercalation, which exfoliates the graphite due to expansion. Currently, the most suitable solvents for LIBs are based on alkyl carbonates such as ethylene carbonate. Although low-melting-point propylene carbonate (PC) exhibits good ionic conductivity over a wide temperature range, its use in LIBs is limited because of its destructive behavior toward the graphite cathode. The mechanism for the destructive behavior of PC is still a subject of intense study.[21−25] Several works have proposed that it is due to the cointercalation of PC with Li^+ to form a ternary graphite intercalation compound, which exerts considerable interlayer stress at the grain boundary of the graphite interlayers and results in its fragmentation.[24−26] According to Buqa et al.,[26] PC has a different electrochemical reactivity on the graphite surface in comparison with ethylene carbonate (EC) and acyclic carbonates. The decomposition products of PC intercalation compounds formed upon its reduction are not able to form an effective solid electrolyte interface (SEI) that passivates the graphite from further solvent cointercalation, thus resulting in the electrochemical exfoliation of the graphite. With regard to LIB applications, the destructive behavior of Li^+/PC toward graphite is an unwanted reaction, as it results in the loss of reversible Li storage capacity. However, we have discovered that the destructive behavior of the Li^+/PC complexes can be exploited for the high-yield exfoliation of graphite to produce FLG flakes.

As illustrated in Scheme 1, graphite was used as the negative electrode in an electrochemical cell. Unlike the low-voltage (<1 V) and low-current electrochemical charging conditions typically used in graphite intercalation compounds (GICs),[21,22] here we applied a high potential (-15 ± 5 V) in order to activate Li/PC cointercalation in graphite. Electrospray ionization mass spectrometry (ESI-MS) analysis of the expanded graphite electrode revealed the presence of the cointercalated Li−PC

Received: April 22, 2011
Published: May 10, 2011

dx.doi.org/10.1021/ja203725d | J. Am. Chem. Soc. 2011, 133, 8888–8891

Scheme 1. Exfoliation of Graphite into Few-Layer Graphene Flakes via Intercalation of Li^+ Complexes[a]

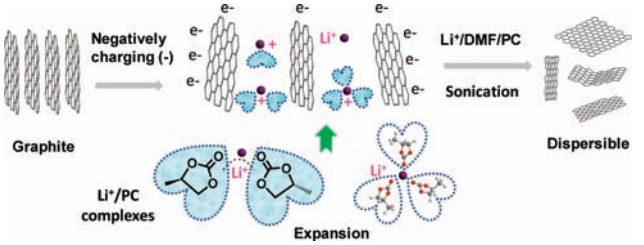

[a] Graphite was electrochemically charged in Li^+/PC using high voltage. The expanded graphite was then exfoliated by power sonication in LiCl in a DMF/PC mixed solvent.

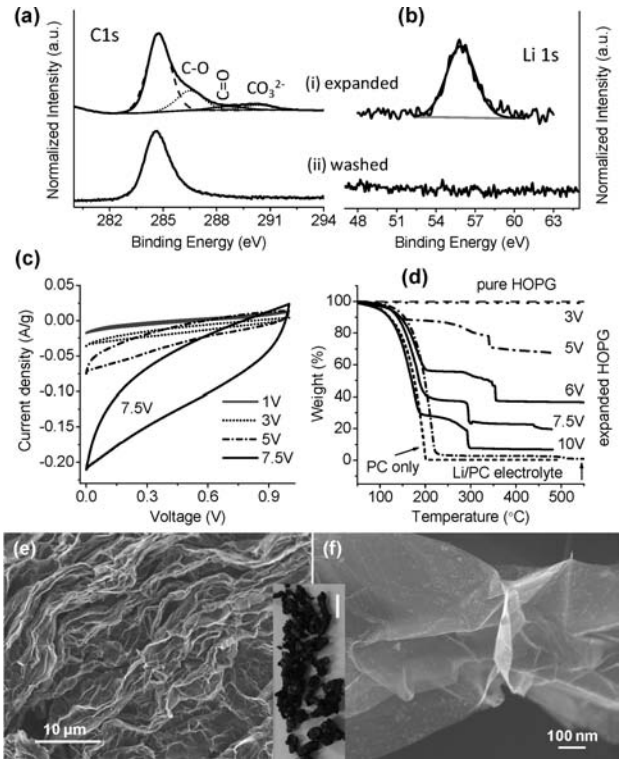

Figure 1. (a, b) XPS narrow scan of C 1s and Li 1s for (i) an expanded HOPG electrode and (ii) after washing of (i) with HCl (1.0 mol/L) and water. (c) Cyclic voltammograms recorded between 0 and 1.0 V at a scan rate of 0.05 V/s after the graphite electrode as the negative electrode had been precharged at potentials of 1, 3, 5, and 7.5 V for 60 min. The electrochemical cell consisted of the graphite electrode, a Li metal electrode, and 30 mg/mL $LiClO_4$ in PC. (d) TGA of expanded graphite under a N_2 atmosphere at different charging voltages. TGA data for graphite, PC, and 30 mg/mL $LiClO_4$ in PC (Li/PC) are shown for comparison. (e, f) SEM images of the expanded HOPG electrode (charged at 7.5 V) after performing TGA (annealed at the rate of 10 °C/min to 500 °C under a N_2 gas flow). The inset shows a photograph of the expanded HOPG after annealing. Scale bar: 5 mm.

complex. ESI-MS analysis of a charged solution of 100 mg/mL $LiClO_4$ in PC identified various Li—PC complexes, as peaks at m/z 210.9 and 312.5 associated with $(Li\cdot 2PC)^+$ and $(Li\cdot 3PC)^+$, respectively, were observed. X-ray photoelectron spectroscopy (XPS) analysis of the exfoliated graphene sheets showed the presence of Li and PC on the graphene sheets (Figure 1a,b), as

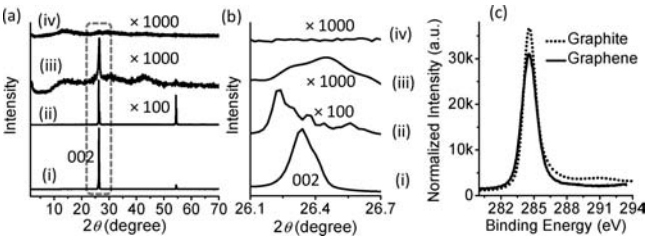

Figure 2. (a, b) XRD spectra: (a) (i) HOPG, (ii) HOPG expanded by Li^+/PC charging, (iii) FLG flakes obtained after one cycle of charging and sonication (>70% are FLG and <30% are thin graphite)and (iv) FLG flakes after three cycles of charging and sonication (>90% FLG); (b) 2θ angle of 26.1—26.7°. (c) XPS C 1s data for graphene and HOPG.

indicated by the chemically shifted components in the C 1s XPS spectrum, which are assignable to oxygenated groups in PC, as well as the presence of the Li 1s elemental XPS peak.

The application of a high charging voltage aids the expansion of the electrode by Li—PC complexes. Under high-voltage, high-current electrochemical charging, the organic solvent decomposed on the cathode, and gas evolution of propylene was detected. Figure 1c shows that the capacitive current of the expanded graphite electrode increased with the charging voltage applied during the electrochemical expansion. Furthermore, thermogravimetric analysis (TGA) of the expanded graphite electrode (Figure 1d) revealed a significant amount of PC intercalation in the graphite electrode after it was charged at high current density. The line trace showing the sharp thermal decomposition step of pure PC in the TGA spectrum in Figure 1d provides a good reference for judging the relative content of intercalated PC in the graphite electrode. For example, at a charging voltage of 7.5 V, the expanded graphite exhibited up to 60% weight loss in TGA. The thermal decomposition profile of the expanded graphite electrode is attributable to the incorporated PC, which ultimately expanded the graphite and destroyed the long-range structure along the c axis. From Figure 1d, we can infer that the amount of PC incorporated in the graphite electrode increases with the charging voltage applied, which clearly indicates that these organic intercalants originated from the electrochemical processes and not from random process such as coprecipitation of organic contaminants when the graphite electrode was collected for analysis. Scanning electron microscopy (SEM) imaging of the thermally annealed electrode revealed graphene-like sheets (Figure 1e,f), which result from the gas expansion of graphite layers following the decomposition of PC. The expanded graphite particles were black (Figure 1e,f inset), and each particle had an electrical conductivity of <10 Ω when measured with hand-held multimeter, indicating that a nonoxidative expansion process produced this conducting material.

The expanded graphite was sonicated in concentrated LiCl dissolved in PC and *N*,*N*-dimethylformamide (DMF) using high-intensity ultrasound. Ultrasonic cavitation injects thermal shock and results in both exfoliation and cutting of the graphene sheets.[27] Removal of the interacalated Li^+/PC was achieved by washing with acid and water.[28,29] XPS analysis of the washed graphene sheets revealed a sharp C 1s peak characteristic of single-phase, pristine graphene (Figure 2c).

We discovered that even in the absence of electrochemical charging, graphite could be exfoliated after sonication for an extended period of time in a solution of LiCl in a mixed solvent of DMF[30,31] and PC. In the absence of Li^+ ions, the exfoliation yield

dx.doi.org/10.1021/ja203725d | J. Am. Chem. Soc. 2011, 133, 8888–8891

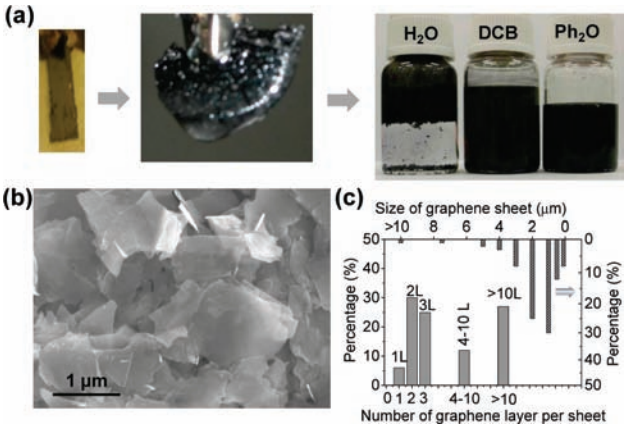

Figure 3. (a) Photographs of (left) HOPG used as a cathode; (center) HOPG after electrochemical intercalation, where it expanded by >50 times in volume; and (right) after sonication of the expanded HOPG to produce FLG, which was dispersed (1 mg/mL) in water, dichlorobenzene (DCB), and diphenyl ether (Ph_2O). (b) Low magnification SEM image. (c) Thickness and size distribution histograms of the FLG produced, as estimated from AFM analysis of the FLG flakes.

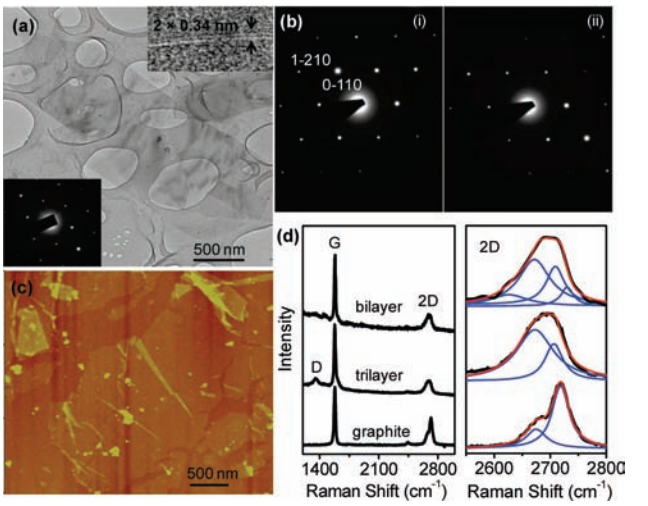

Figure 4. (a) TEM images and electron diffraction pattern for FLG. (b) Electron diffraction patterns of (i) single and (ii) bilayer sheets. (c) AFM image of FLG spin-coated onto a Si substrate. The thickness was ~1.5 nm, corresponding to a bilayer. (d) (left) Raman spectra (532 nm laser) of FLG on Si substrates compared with the spectrum of graphite; (right) Lorentzian peak fitting of the 2D bands of the bilayer and trilayer.[32−34].

was less than <1%, and only small-sized graphene flakes were obtained (Table S1 in the Supporting Information). This suggests that Li^+ ions in the organic solvent play an important role in the exfoliation of graphite.

The exfoliated graphene flakes were examined by X-ray diffraction (XRD) to assess whether the long-range periodicity associated with the *c* axis in thick graphite had been modified (Figure 2a,b and Figure S1 in the Supporting Information). In fact, after the graphite was electrochemically charged in Li^+/PC, it expanded considerably and the (002) reflection characteristic of the $\pi-\pi$-stacked layers was noticeably weakened (Figure 2a,b). The (002) peak decreased by several order of magnitude after one cycle of charging and sonication and vanished after three charging/sonication cycles. These hydrophobic FLG flakes float on a water surface and can be dispersed in dichlorobenzene and diphenyl ether (1 mg/mL), as shown in Figure 3a (right).

The exfoliated FLG could be imaged clearly by SEM without the charging problems that usually affect GO. Figure 3b and Figure S2 present typical SEM images of the FLG sheets, in which the average lateral dimension of the graphene sheets was 1−2 μm. Analysis of the diffraction spot intensity in transmission electron microscopy (TEM) shed some light on the thickness of these graphene layers. A monolayer graphene film is distinguished by a stronger diffraction intensity from the $(0\bar{1}10)$ plane than from the $(1\bar{2}10)$ plane, and the reverse is true for bilayer or trilayer graphene films. Our FLG had stronger diffraction spots from the $\{1\bar{2}10\}$ planes than from the $\{0\bar{1}10\}$ planes. The observed intensity ratio $I\{0\bar{1}10\}/I\{1\bar{2}10\}$ was typically between 2/1 and 1/1.5, which suggests that the layer thickness was 1− 3 layers (Figure 4a,b and Figure S3).[4] On the basis of statistical sampling of the FLG flakes using atomic force microscopy (AFM) (Figure 4c and Figure S4), it was estimated that 50% of the graphene sheets comprised 2−3 layers of graphene (see the size histogram in Figure 3c).

Raman spectroscopy was used to check the crystalline quality of the graphene flakes by monitoring the relative intensity of the D peak (defect-related) and the G peak (doubly degenerate zone center E_{2g} mode). Figure 4d (right) presents the Lorentzian peak fitting[32,33] (for the optical contrast spectra, see Figure S5)[34] of the 2D peak using deconvoluted peaks characteristic of FLG with two and three layers.[32−34] As shown in Figure 4d (left), the I_D/I_G intensity ratio of <0.1 indicates that the concentration of defects in our FLG was significantly lower than that of GO, which typically has a ratio of >0.8.[8] The small D band (1341 cm^{-1}) may be edge-related, as a result of the small size of the flake relative to the size of the Raman probe. On the basis of peak profile and peak position analysis as well as optical contrast spectroscopy of the FLG flakes, we can conclude that >70% of the FLG flakes had thicknesses of <5 layers (Figure S6).[4,32−34] The FLG films transferred onto plastic substrates showed good electrical conductivity versus transparency without any form of annealing or sintering (Figure S7).

The electrochemical charging method developed here can be combined with microwave irradiation to scale up the production of dispersible FLG flakes from graphite powder. Figure 5a shows that gram quantities (15 g) of FLG flakes could be prepared in the laboratory by high-yield exfoliation. A highly dispersible carbon "ink" could be produced by the dispersion of the FLG flakes in several solvents (e.g., 10 mg/mL in DCB), and brush painting could be performed on commercial paper (Figure 5b). The highly porous nature of paper provides a strong capillary force for the FLG ink, and conformal coating of the FLG on paper could be readily achieved, transforming the paper into a conductive sheet (Figure 5b−d).[35] Figure 5e shows the relationship of the paper resistance to the graphene loading amount. When 0.7 mg/cm^2 graphene was loaded, a sheet resistance as low as 15 ohm/□ was obtained, which is better than that of reduced graphene oxide paper[36] and comparable to that of high-quality carbon nanotube-treated paper.[35]

In conclusion, we have devised a high-yield method for producing few-layer graphene (FLG) flakes by electrochemical charging of graphite electrodes in a Li^+/propylene carbonate electrolyte. The yield of FLG (>70%) obtained from the graphite electrode is significantly higher than that produced by most current liquid-phase exfoliation methods. The graphene flakes

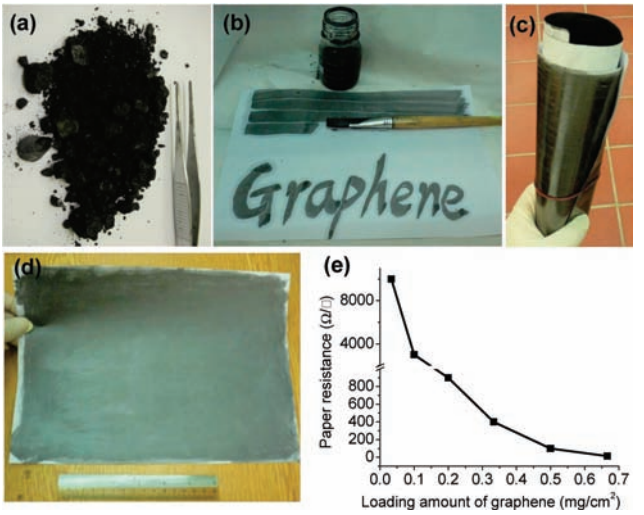

Figure 5. FLG powder and its derived ink that can be used to make highly conductive paper. (a) Photograph of FLG powder (15 g). (b) Ink consisting of FLG in DCB (10 mg/mL) for brushing and writing on common paper. (c, d) Commercial A4 printing paper coated with FLG. (e) Relationship between the resistance of the paper and the graphene loading amount.

can be employed in conducting inks for conformal coatings. The implication is that graphite electrodes used in lithium rechargeable batteries can be recycled to produce FLG flakes by application of a high current density during electrochemical charging in PC followed by sonochemical exfoliation. This approach thus constitutes an industrially scalable processing method for producing conducting graphene flakes from graphite electrodes and is distinct from the many acid exfoliation methods that produce mainly insulating GO derivatives.

■ ASSOCIATED CONTENT

Ⓢ Supporting Information. Characterization methods, additional experimental data, and complete ref 4. This material is available free of charge via the Internet at http://pubs.acs.org.

■ AUTHOR INFORMATION

Corresponding Author
chmlohkp@nus.edu.sg

■ ACKNOWLEDGMENT

The work was funded by the NRF−CRP Grant "Graphene Related Materials and Devices" R-143-000-360-281 and the NUS-Singapore Millenium Foundation Research Horizon Award R-143-000-417-592/646.

■ REFERENCES

(1) Lu, X.; Yu, M.; Huang, H.; Ruoff, R. S. *Nanotechnology* **1999**, *10*, 269.
(2) Li, X.; Wang, X.; Zhang, L.; Lee, S.; Dai, H. *Science* **2008**, *319*, 1229.
(3) Liu, N.; Luo, F.; Wu, H.; Liu, Y.; Zhang, C.; Chen, J. *Adv. Funct. Mater.* **2008**, *18*, 1518.
(4) Hernandez, Y.; et al. *Nat. Nanotechnol.* **2008**, *3*, 563.
(5) Vallés, C.; Drummond, C.; Saadaoui, H.; Furtado, C. A.; He, M.; Roubeau, O.; Ortolani, L.; Monthioux, M.; Pénicaud, A. *J. Am. Chem. Soc.* **2008**, *130*, 15802.
(6) Park, S.; Ruoff, R. S. *Nat. Nanotechnol.* **2009**, *4*, 217.
(7) Cano-Márquez, A. G.; Rodríguez-Macías, F. J.; Campos-Delgado, J.; Espinosa-González, C. G.; Tristán-López, F.; Ramírez-González, D.; Cullen, D. A.; Smith, D. J.; Terrones, M.; Vega-Cantú, Y. I. *Nano Lett.* **2009**, *9*, 1527.
(8) Allen, M. J.; Tung, V. C.; Kaner, R. B. *Chem. Rev.* **2010**, *110*, 132.
(9) Behabtu, N.; Lomeda, J. R.; Green, M. J.; Higginbotham, A. L.; Sinitskii, A.; Kosynkin, D. V.; Tsentalovich, D.; Parra-Vasquez, A. N. G.; Schmidt, J.; Kesselman, E.; Cohen, Y.; Talmon, Y.; Tour, J. M.; Pasquali, M. *Nat. Nanotechnol.* **2010**, *5*, 406.
(10) Novoselov, K. S.; Geim, A. K.; Morozov, S. V.; Jiang, D.; Zhang, Y.; Dubonos, S. V.; Grigorieva, I. V.; Firsov, A. A. *Science* **2004**, *306*, 666.
(11) Geim, A. K. *Science* **2009**, *324*, 1530.
(12) Hummers, W. S., Jr.; Offeman, R. E. *J. Am. Chem. Soc.* **1958**, *80*, 1339.
(13) Gómez-Navarro, C.; Weitz, R. T.; Bittner, A. M.; Scolari, M.; Mews, A.; Burghard, M.; Kern, K. *Nano Lett.* **2007**, *7*, 3499.
(14) Stankovich, S.; Dikin, D. A.; Dommett, G. H. B.; Kohlhaas, K. M.; Zimney, E. J.; Stach, E. A.; Piner, R. D.; Nguyen, S. T.; Ruoff, R. S. *Nature* **2006**, *442*, 282.
(15) Stankovich, S.; Dikin, D. A.; Piner, R. D.; Kohlhaas, K. A.; Kleinhammes, A.; Jia, Y.; Wu, Y.; Nguyen, S. T.; Ruoff, R. S. *Carbon* **2007**, *45*, 1558.
(16) Liang, Y.; Wu, D.; Feng, X.; Müllen, K. *Adv. Mater.* **2009**, *21*, 1679.
(17) Viculis, L. M.; Mack, J. J.; Kaner, R. B. *Science* **2003**, *299*, 1361.
(18) Li, X.; Zhang, G.; Bai, X.; Sun, X.; Wang, X.; Wang, E.; Dai, H. *Nat. Nanotechnol.* **2008**, *3*, 538.
(19) Lotya, M.; Hernandez, Y.; King, P. J.; Smith, R. J.; Nicolosi, V.; Karlsson, L. S.; Blighe, F. M.; De, S.; Wang, Z.; McGovern, I. T.; Duesberg, G. S.; Coleman, J. N. *J. Am. Chem. Soc.* **2009**, *131*, 3611.
(20) Choucair, M.; Thordarson, P.; Stride, J. A. *Nat. Nanotechnol.* **2009**, *4*, 30.
(21) Chung, G. C.; Kim, H. J.; Yu, S. I.; Jun, S. H.; Choi, J.; Kim, M. H. *J. Electrochem. Soc.* **2000**, *147*, 4391.
(22) Dresselhaus, M. S.; Dresselhaus, G. *Adv. Phys.* **2002**, *51*, 1.
(23) Xu, K. *Chem. Rev.* **2004**, *104*, 4303.
(24) Wagner, M. R.; Albering, J. H.; Moeller, K. C.; Besenhard, J. O.; Winter, M. *Electrochem. Commun.* **2005**, *7*, 947.
(25) Abe, T.; Mizutani, Y.; Kawabata, N.; Inaba, M.; Ogumi, Z. *Synth. Met.* **2001**, *125*, 249.
(26) Buqa, H.; Würsig, A.; Vetter, J.; Spahr, M. E.; Krumeich, F.; Novák, P. *J. Power Sources* **2006**, *153*, 385.
(27) Suslick, K. S.; Price, G. *Annu. Rev. Mater. Sci.* **1999**, *29*, 295.
(28) Arakawa, M.; Yamaki, J. I. *J. Electroanal. Chem.* **1987**, *219*, 273.
(29) Zhu, Y.; Stoller, M. D.; Cai, W.; Velamakanni, A.; Piner, R. D.; Ruoff, R. S. *ACS Nano* **2010**, *4*, 1227.
(30) Piret, P. *Bull. Soc. Chim. Fr.* **1962**, 1981.
(31) Rao, C. P.; Rao, A. M.; Rao, C. N. R. *Inorg. Chem.* **1984**, *23*, 2080.
(32) Ferrari, A. C.; Meyer, J. C.; Scardaci, V.; Casiraghi, C.; Lazzeri, M.; Mauri, F.; Piscanec, S.; Jiang, D.; Novoselov, K. S.; Roth, S.; Geim, A. K. *Phys. Rev. Lett.* **2006**, *97*, 187401.
(33) Graf, D.; Molitor, F.; Ensslin, K.; Stampfer, C.; Jungen, A.; Hierold, C.; Wirtz, L. *Nano Lett.* **2007**, *7*, 238.
(34) Ni, Z. H.; Wang, H. M.; Kasim, J.; Fan, H. M.; Yu, T.; Wu, Y. H.; Feng, Y. P.; Shen, Z. X. *Nano Lett.* **2007**, *7*, 2758.
(35) Hu, L.; Choi, J. W.; Yang, Y.; Jeong, S.; Mantia, F. L.; Cui, L.-F.; Cui, Y. *Proc. Natl. Acad. Sci. U.S.A.* **2009**, *106*, 21490.
(36) Dikin, D. A.; Stankovich, S.; Zimney, E. J.; Piner, R. D.; Dommett, G. H. B.; Evmenenko, G.; Nguyen, S. T.; Ruoff, R. S. *Nature* **2007**, *448*, 457.